

NOVEL FIBER OPTIC SENSOR BASED ON IN-LINE CORE-CLADDING INTERMODAL INTERFEROMETER AND PHOTONIC CRYSTAL FIBER

Wojtek J. Bock,¹ Tinko Eftimov,² Predrag Mikulic¹ and Jiahua Chen¹

¹Université du Québec en Outaouais, Gatineau, Québec, Canada

²Plovdiv University “P. Hilendarski” Plovdiv 4000, Bulgaria

Abstract – We propose a simple all-fiber structure based on intermodal interference between a core and a cladding mode of an endlessly single-mode photonic crystal fiber section sandwiched between a lead-in and lead-out SMF-28 fiber. The sensitivities to strain, pressure and temperature are measured. The interferometer is compared to an interferometer based on LP₀₁-LP₀₂ SMF-28 fiber and to a PCF-based tapered LPG.

Keywords: intermodal interferometer, photonic crystal fiber, fiber-optic sensors.

1. INTRODUCTION

Recently, several works have appeared on the development of a novel type of sensor using intermodal interference between forward-propagating core and cladding modes along a microstructured optical fiber (MOF) [1-2] or along a photonic crystal fiber (PCF) [3].

Unlike conventional intermodal sensors in standard optical fibers [4] or in PCFs [5], core-cladding mode interference sensors exhibit sensitivity not only to strain, temperature and pressure, but very much like long-period gratings (LPGs) [6], are also sensitive to bending, torsion and most importantly to ambient refractive index changes. Therefore, one of the first applications was for hydrogen concentration sensing [1] in combination with thin palladium layers deposited on a collapsed MOF fiber section. Strain sensing has also been investigated [2-3]. Three different fabrication techniques have been suggested and tested. One is to collapse a section of the MOF and form a tapered region [1] which becomes a glass-air waveguide supporting interfering higher-order modes [7]. The second is to splice an MOF sensing section between two other MOF pieces [2] or to just collapse the holes at two different positions [3]. In the spliced regions, the holes of the MOF collapse and the structure becomes a glass-air waveguide, in which higher-order modes are excited and propagated along the sensing section. A third method [3] is to use lateral offset splicing between the lead-in / lead-out and the sensing fibers. Depending on the offset, different higher-order modes can be excited. In all these cases, both the lead-in/lead-out and the sensing fibers have been of the same type. Unless endless single-mode operation is needed, using MOS/PCF fibers as lead-in and lead-out fibers is highly inefficient and expensive.

In this paper we present a simpler and more cost-effective method for the construction of an in-line core-cladding intermodal interferometer based on the use of abrupt tapers formed at the splices between lead-in and lead-out standard SMF-28 fibers and an endlessly single-mode PCF fiber sandwiched in between them. These fibers are characterized by different core and mode field diameters which create the abrupt tapers.

We have tested the sensor for sensitivity to strain, pressure and temperature as well as external refractive index and have compared its sensitivity with standard core-mode LP₀₁-LP₀₂ intermodal interferometers on the one hand, and with PCF-based LPGs on the other.

2. CORE-CLADDING INTERMODAL INTERFEROMETER USING PCF

2.1. Structure and output spectral response

The all-fiber structure is shown in Fig. 1. A piece of endlessly single-mode PCF (ESM-12-01) is spliced between a lead-in and a lead-out SMF-28 fiber.

The PCF fiber section is stripped off from the polymer coating, so that the outer refractive index is that of air. In such a structure, higher-order cladding modes of the PCF fiber, which would otherwise be radiated through the polymer cladding, are now guided, the surrounding medium (air) acting as a low-refractive-index cladding.

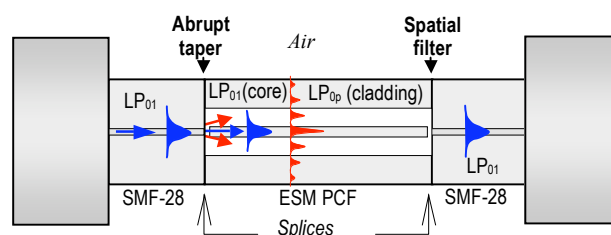


Fig. 1 Schematic representation of the core-cladding intermodal interferometer based on the mode-field mismatch method. The abrupt tapers are formed at the splices between two dissimilar fibers such as the standard SMF-28 and the endlessly single-mode PCF.

Looking at the data in Table 1, we notice that the diameter of the fundamental LP₀₁ mode in the SMF-28 fiber is $w_{SMF} = 9.2 \mu\text{m}$ whereas in the PCF $w_{PCF} = 6.4 \mu\text{m}$. We thus obtain an abrupt change of the waveguide properties,

which means that at the splice we have an abrupt taper. Also, as shown in [2], the fundamental mode field coming out of the SMF will broaden due to diffraction in the region of collapsed holes. For this reason, the LP_{01} mode distribution of the SMF-28 fiber cannot adapt smoothly to the LP_{01} mode distribution of the PCF fiber and couples part of its power to higher-order cladding modes of the PCF fiber. Normally, if the PCF fiber is polymer-coated these modes will exhibit high loss. If the PCF section is stripped, however, these cladding modes are better guided and their fields overlap with the field of the fundamental LP_{01} core-mode. We then will observe interference between a core and a cladding mode. At the second splice we have another abrupt taper and the SMF-28 lead-out fiber does not support the higher-order cladding mode. Whatever cladding modes are excited get quickly attenuated, so the second SMF-28 fiber section acts as a spatial filter for the intermodal interference pattern. We thus have an all-fiber core-cladding intermodal interferometer in an in-line Mach-Zender arrangement.

Table 1. Parameters of the SMF-28 fiber and the ESM-12-01-PCF

Parameter [μm]	SMF-28	ESM-12-01-PCF
Mode field diameter	9.2 ± 0.4	6.4 ± 0.2
Core diameter	8.2	12.0 ± 0.1
Cladding diameter	125 ± 1	125 ± 1
Holey region diameter	N.A.	57.4 ± 1

There are two important features of the present LP_{01} - LP_{0p} interferometer compared to core-core intermodal interferometers. The first is that it shows very low temperature sensitivity since the PCF fiber is made of a single material. The second is that, since one of the interfering modes is a cladding higher-order mode, its effective refractive index, and consequently its propagation constant, will be very sensitive to the refractive index of the surrounding medium.

We fabricated several samples of all-fiber SMF-PCF-SMF structures as shown in Fig. 2, establishing lengths of the PCF section from $L = 5$ mm to $L = 53$ mm. The sample having the PCF section with $L = 44$ mm was subjected to different tests.

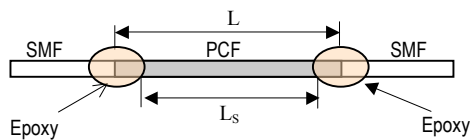


Fig. 2 Structure of the sensor

Using an ASE broadband source and an Ando AQ6315A OSA, the spectral response of the intermodal sensor was taken and the periodic structure is shown in Fig. 3.

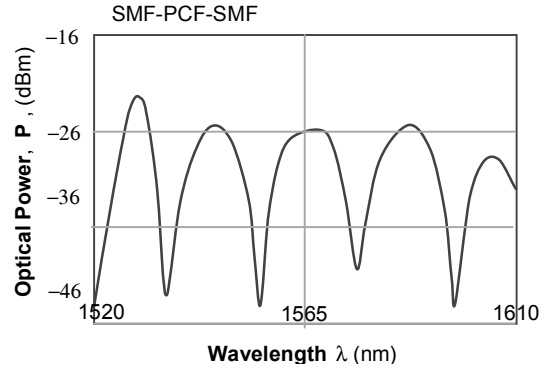
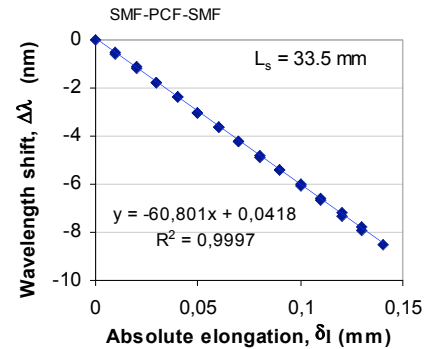


Fig. 3 Spectral response of an intermodal sensor

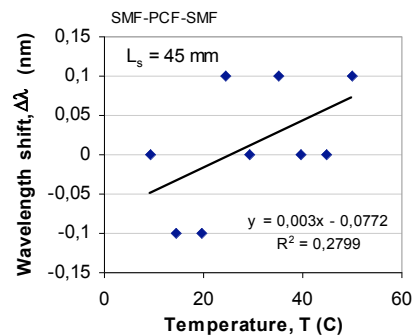
2.2. Experiment and results

Fig. 2 shows the dimensions of the sensor arrangement for strain sensing. Because of the epoxy area covering the splices, the active sensing length is reduced from 44 mm to $L_s = 33.5$ mm.

We measured the wavelength shift at 1604 nm from Fig. 3 caused by elongation and the results are plotted in Fig. 4(a). Similarly to LPGs, the sensitivity to strain has a negative coefficient, which means that the interference pattern moves left to lower wavelengths and for the sensing length of $L_s = 33.5$ mm the sensitivity was found to be $d\lambda/dl = -60.801$ nm/mm.



(a) Minimum wavelength shift under elongation



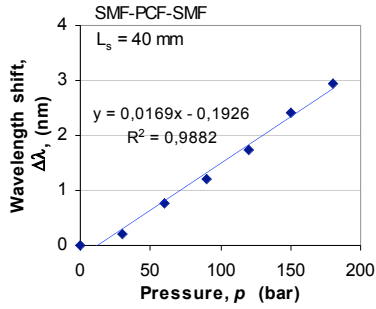
(b) Temperature effect

Fig. 4 Response to elongation

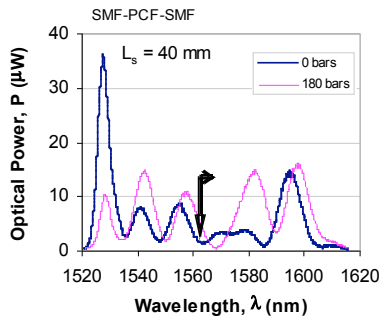
Measurement of temperature sensitivity was performed on a third sensor with $L_s = 45$ mm. The wavelength shift of

its first minimum is shown in Fig. 4(b). The sensitivity to temperature was found to be in the order of $d\lambda/dT = 3 \text{ pm/K}$.

The sensitivity to pressure was measured after we installed another sensor with length $L_s = 40 \text{ mm}$ in a high-pressure chamber. The wavelength shifts vs. pressure are shown in Fig. 5(a) and the sensitivity was found to be $d\lambda/dp = 16.9 \text{ pm/bar}$. During pressure changes, the spectrum of the sensor moved to higher wavelengths and also changed shape as can be seen from Fig. 5(b).



(a) Minimum wavelength shift under pressure



(b) Spectrum response to pressure

Fig. 5 Response to hydrostatic pressure

As is also evident from Fig. 5, the different minima shift to different wavelengths. There are two reasons for this. The first is the presence of more than one higher-order cladding mode excited at the splice, which leads to multiple instances of intermodal interference. This problem can be eliminated by placing the cladding in an immersion liquid with a suitable refractive index or, if this is inappropriate, by etching part of the cladding to increase the spacing between the higher-order modes. The second reason for the shift to different wavelengths is the existence of polarization dependence of the intermodal interference. This polarization sensitivity arises in the collapsed regions at the splices where the holes of the PCF fiber become elliptic in shape with random orientation, which, in turn causes random parasitic birefringence.

Since the higher-order mode is a cladding mode of a glass-air waveguide, any change of the outer refractive index caused by immersion in a liquid will change the propagation constant of the higher-order mode and consequently cause a shift in the interference fringes. Given that the sensors have to be inserted into a liquid for pressure measurements, the sensitivity to refractive index for the

transition air-water has been evaluated. Fig. 6 shows a comparison of the spectral responses in air ($n = 1$) and in water ($n = 1.3352$) for an interferometer whose length is $L = 50 \text{ mm}$.

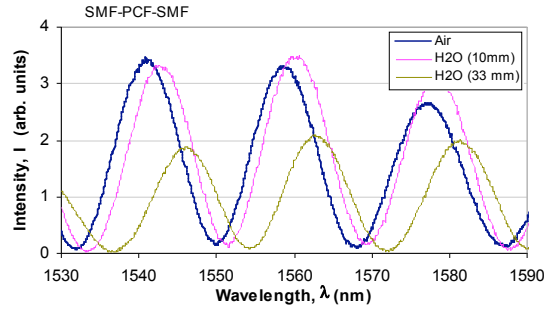


Fig. 6 Spectral response to external refractive index

The two responses in water correspond to sensing lengths of $L_s = 10 \text{ mm}$ and $L_s = 33 \text{ mm}$. For the 33 mm sensing length, the wavelength shift was $\delta\lambda = 5 \text{ nm}$ per refractive index change of $\delta n = 1.3352 - 1 = 0.3352 \text{ r.i.u}$ (refractive index units). Since the 2π spectral period is $\Delta\lambda_{2\pi} = 18.2 \text{ nm}$, then we can find that $T_n = 1.22 \text{ r.i.u.}$ and the corresponding sensitivity is $\Lambda_n = 5.14 \text{ rad/r.i.u.}$ The $T_n \times L_s$ product can then be calculated as $4.03 \times 10^{-3} \text{ r.i.u.} \times \text{m}$.

In the refractive index range from 1.33 to 1.38, $T_n = 0.18 \text{ r.i.u.}$ ($\Lambda_n = 34.88 \text{ rad/r.i.u.}$) and in the range from 1.38 to 1.46, $T_n = 0.027 \text{ r.i.u.}$ ($\Lambda_n = 230 \text{ rad/r.i.u.}$) as summarized in Table 2. Thus, as with LPGs, sensitivity dramatically increases as the external refractive index approaches that of the cladding.

It is worth comparing the present sensor with conventional SMF-28-based LP_{01} - LP_{02} intermodal sensors as well as with PCF-based LPGs.

Table 2 compares the present PCF-based core-cladding mode interference sensor and an earlier SMF-28-based core-core mode interference sensor. The sensitivity is expressed in terms of the $T_\xi \times L_s$ product which is a constant quantity. We see that this PCF intermodal sensor is about 40 times less sensitive to temperature (which is important for temperature compensation), 9.3 times less sensitive to strain and about 5.8 times more sensitive to pressure.

Table 2. Comparison of responses between the present LP_{01} - LP_{0p} PCF-based interferometer and a previous LP_{01} - LP_{02} SMF-based intermodal interferometer.

Parameter	$T_\xi \times L_s$ product	LP_{01} - LP_{0p} PCF-based	LP_{01} - LP_{02} SMF-based
Temperature	$T_T \times L_s$ (Kxm)	305.87	7.75
Strain	T_ϵ ($\mu\epsilon$)	9 850.8	1 058
Pressure	$T_p \times L_s$ (bar x m)	32.9	190
Refractive index	$T_n \times L_s$ (r.i.u. x m) ($L_s = 33 \text{ mm}$)	$4.03 \cdot 10^{-3}$ ($n = 1.00$ to 1.33) $5.94 \cdot 10^{-3}$ ($n = 1.33$ to 1.38) $8.91 \cdot 10^{-4}$ ($n = 1.38$ to 1.46)	---

Table 3 compares the same PCF-based core-cladding mode interference sensor and a PCF-based tapered LPG (TLPG) reported in [8]. The TLPG's sensing length is $L_s = 40$ mm, while the lengths of the PCF core-cladding intermodal sensor vary between 33 mm and 45 mm as indicated in parentheses.

Table 3. Comparison of responses between the present LP_{01} - LP_{0p} PCF-based interferometer and PCF-based tapered LPGs.

Parameter	$d\lambda/d\chi$	LP_{01} - LP_{0p} PCF-based	PCF Tapered LPG
Temperature	$d\lambda/dT$ (pm/K)	< 3 ($L_s = 45$ mm)	0.3 ($L_s = 40$ mm)
Strain	$d\lambda/dl$ (pm/ $\mu\epsilon$)	- 2.04 ($L_s = 33.5$ mm)	- 4.29 ($L_s = 40$ mm)
Pressure	$d\lambda/dp$ (pm/bar)	16.9 ($L_s = 40$ mm)	11.2 ($L_s = 40$ mm)
Refractive index	$d\lambda/dn$ (nm/r.i.u.) ($L_s = 33$ mm)	14.90 (n = 1.00 to 1.33) 99.37 (n = 1.33 to 1.38) 700 (n = 1.38 to 1.46)	----

This PCF-based TLPG pressure sensor [8] functions in reflective configuration, so that light passes twice along the same LPG. The TLPG length being 20 mm, the effective sensing length then becomes $L_s = 40$ mm with a reported sensitivity to pressure $d\lambda/dp = 11.2$ pm/bar. For the same sensing length, the LP_{01} - LP_{0p} intermodal PCF-based sensor shows a sensitivity of $d\lambda/dp = 16.9$ pm/bar which is an increase of 50% at a temperature sensitivity of less than 3pm/K. Sensitivity to strain is negative and about 2.1 times lower than that of the PCF TLPG sensor. Compared to LPGs, sensitivity to refractive index changes is lower but covers a wider range. Thus with the intermodal interferometer we obtain practically constant sensitivity of 700 nm/r.i.u. for $n = 1.38$ to 1.46, versus almost 10 times as much for the range from $n = 1.44$ to 1.445 [6]. More detailed results on refractive index sensitivity of core-cladding intermodal interferometers will be presented in another publication.

The two comparisons show that the type of sensor discussed here is best suited for temperature-insensitive pressure and strain sensing. One disadvantage is the higher splice losses.

On the positive side, the major advantage compared to LPGs is that the sensitivity can be increased by increasing the sensing length. In this case, maxima will be closer to one another and wavelength shifts can be measured with greater accuracy.

3. CONCLUSIONS

We have fabricated and tested a simple and cost-effective core-cladding mode interferometer based on an endlessly single-mode PCF fiber spliced between lead-in and lead-out standard SMF-28 fibers. The interferometer is sensitive to pressure, strain and ambient refractive index

changes as well as to bending. It shows a 5 times greater sensitivity to pressure than a core-core intermodal sensor based on SMF-28 fiber and 50% higher sensitivity than a tapered PCF-based LPG. As the sensing fiber is a photonic crystal one, temperature sensitivity is very low. This type of sensor features the typical advantages of PCF-based LPGs but its sensitivity can be increased by increasing the sensor length.

ACKNOWLEDGMENTS

The authors gratefully acknowledge support for this work from the Natural Sciences and Engineering Research Council of Canada and from the Canada Research Chairs Program.

REFERENCES

- [1] V. P. Minkovich, D. Monzón-Hernández, J. Villatoro and G. Badenes, "Microstructured optical fiber coated with thin films for gas and chemical sensing", *Opt. Express*, Vol. 14, pp. 8413-8418, September 2006.
- [2] J. Villatoro, V. P. Minkovich, V. Pruneri and G. Badenes, "Simple all-microstructure optical-fiber interferometer built via fusion splicing". *Opt. Express*, Vol. 15, pp. 1491-1496, February 2007.
- [3] H. Y. Choi, M. J. Kim and B. H. Lee, "All fiber Mach-Zender type interferometers formed in photonic crystal fiber", *Opt. Express*, Vol. 15, No. 9, 5711-5720, April 2007.
- [4] T. A. Eftimov and W. J. Bock, "Sensing with a LP_{01} - LP_{02} intermodal interferometer", *J. Lightwave Techn.*, Vol. 11, No. 12, pp. 2150-2156, December 1993.
- [5] D. Káčik, I. Turek, I. Martinček, J. Canning, N. Issa and K. Lyytikäinen, "Intermodal interference in photonic crystal fiber," *Opt. Express*, Vol. 12, pp. 3465-3470, July 2004.
- [6] V. Bhatia, "Applications of long-period gratings to single- and multi-parameter sensing", *Opt. Express*, Vol. 4, No. 11, pp. 457-466, May 1999.
- [7] S. Lacroix, R. Bourbonnais, F. Gonthier and J. Bures, "Tapered monomode optical fibers: Understanding large power transfer", *Appl. Opt.*, Vol. 25, No. 23, pp. 4421-4425, December 1986.
- [8] W. J. Bock, J. Chen, P. Mikulic and Michal Pawlowski, "Pressure sensing using periodically tapered long-period gratings written in photonic crystal fibers", *Meas. Sci. Technol.*, Vol. 18, pp. 3098-3012, 2007.